Indian Journal of Chemistry
Vol. 59A, September 2020, pp. 1305-1312

Benzimidazolium picrate single crystal: Synthesis, growth, characterization and their biological activity

Ganesan Vadivelan[a], Grahandurai Gohulavani[b]*, Munusamy Saravanabhavan[c], Venkatesan Murugesan[d] & Marimuthu Sekar[c]

[a]Department of Chemistry, Kongunadu Arts and Science College, Coimbatore, Tamil Nadu, India
[b]Department of Chemistry, Ethiraj College for Women, Chennai, Tamil Nadu, India
[c]Department of Chemistry, Sri Ramakrishna Mission Vidyalaya College of Arts and Science, Coimbatore, Tamil Nadu, India
[d]Krishna Arts and Science College, Krishnagiri, Tamil Nadu, India
*E-mail:gohulavanigg@gmail.com

Received 10 April 2020; *accepted 26 July 2020*

Knowledge on charge-transfer complexes of drugs is important to understand the drug-receptor binding mechanism. Here, we have been synthesized the organic charge transfer complex of Benzimidazolium picrate (BP) and confirmed its molecular structure and carbon skeleton by ^{1}H and ^{13}C NMR spectral analysis. Asymmetric unit of BP consists of one benzimidazolium cation and a monovalent anion of picric acid. Decomposition pattern and thermal stability BP have been investigated using TG/DTA analysis. The interaction of the compound with calf thymus DNA is investigated by electronic absorption spectroscopy which indicates that the compound could interact with DNA through intercalation. The CT complex demonstrated significant free radical scavenging with 2,2-diphenyl-2-picryl-hydrazyl. The BP complex has been also screened for its antimicrobial activity.

Keywords: Benzimidazolium picrate, Charge-transfer complex, 2,2-Diphenyl-2-picryl-hydrazyl

All heterocyclic compounds have high significance in pharmaceutical chemistry. The benzimidazole moiety is bicyclic, consisting of fusion of benzene and imidazole, and is widely used in designing new drugs[1]. The benzimidazole derivatives represent one of the most biologically active class of compounds, possessing a wide spectrum of activities[2,3]. The benzimidazole nucleus has significance in medicinal chemistry, and many benzimidazole-containing compounds exhibit important biological activities viz. selective neuropeptide YY1 receptor antagonists, 5- lipoxygenase inhibitors for use as novel anti-allergic agents[4], factor Xa (FXa) inhibitors[5], poly (ADP-ribose) polymerase (PARP) inhibitors[6] and as human cytomegalovirus (HCMV) inhibitors[7]. The structural resemblance of benzimidazole nucleus to biological compounds, such as the purine base of the DNA and the occurrence of this nucleus in vitamin B12 are of interest in pharmaceutical industry[8-12]. Benzimidazole constitutes an important group of electron donor or proton acceptor and the study of their charge transfer complex can help elucidate many chemical phenomena[13-17].

Proton or charger transfer complexes play an important role in the field of magnetic, electrical conductivity and optical properties[18-22]. The crystalline charge transfer complexes (CTCs) are known to have a vital role in biological systems such as antimicrobial activity and DNA-binding as well as in laser technology, optoelectronics, optical communications, photocatalyst, optical signal processing and dendrimer fabrication for drug delivery systems[23-32].

CT-interactions between aromatic electron acceptors and electron donors containing nitrogen, oxygen or sulphur atoms have been reported over the previous year[33-36]. Picric acid forms crystalline picrate salts with various organic molecules by virtue of its Lewis acid behaviour and serve as a better acidic ligand in the formation of salts through specific electrostatic or hydrogen bonding interactions[37]. Hence benzimidazole acts as the electron donor and picric acid acts as electron acceptor. Based on the above significance, sincere attempts were made for the successful synthesis of BP crystal. The current research work focuses on the UV-absorption and NMR characterisation, single crystal X-ray diffraction study of the BP crystal. In addition the DNA binding, antimicrobial activity and cleavage activities of the synthesised crystal were also investigated in detail.

Materials and Methods

All the chemicals used were chemically pure and are AR grade. Solvents were purified and dried according to the standard procedures[38]. Calf-thymus (CT-DNA) was purchased from Genei, Bangalore, India. Tetracycline, Nystatin and Agar were purchased from Hi-Media, Mumbai.

Physical characterisation techniques

Micro analyses (C, H and N) were performed on a Vario EL III CHNS analyzer at STIC, Cochin University of Science and Technology, Kerala, India. The IR spectrum was recorded employing KBr pellet method in the region of 400–4000 cm^{-1} using a PerkinElmer FTIR 8000 spectrophotometer. Electronic spectrum was recorded in methanol solution with a Systronics double beam UV–visible spectrophotometer 2202 in the range 200–800 nm. ^{1}H and ^{13}C NMR spectra were recorded on a Bruker AV III 500 MHZ instrument using TMS as an internal reference at SAIF, Indian Institute of Technology, Madras. Melting points were recorded with Veego VMP-DS heating table and are uncorrected. The thermal analysis (TG and DTA) were carried out under nitrogen atmosphere with a heating rate of 20°C/ min by NETZCHSTA 409C analyzers. DNA cleavage study was carried out using Gelstan - Gel documentation system. Antioxidant study was carried out at the Kovai Medical Centre and Hospital Pharmacy College, Coimbatore, Tamil Nadu, India.

X-ray crystal structure determination

The crystallographic data of the complex has been measured at 298 K on a Bruker SMART APEX CCD, area detector system [λ (MoKα) =0.71073 Å]. A graphite monochromator, 2400 frames was recorded with an ω scan width of 0.3°, each for 10 s, crystal-detector distance 60 mm, collimator 0.5 mm. Data reduction was carried out by SAINPTUS[39] and absorption correction was made using an empirical method SADBS[40]. The structure was studied and refined using SHELXL-97[41]. All non hydrogen is refined anisotropically. Cambridge Crystallographic Data Centre (CCDC No.1019637) contains the supplementary crystallo-graphic data for the complex.

Synthesis of Benzimidazolium picrate (BP) complex

Equimolar ratio of benzimidazole in methanol and picric acid in water were dissolved and mixed together. The solution was stirred well for about 2 h at room temperature using magnetic stirrer to ensure homogeneous mixture, filtered using Whatmann 41 filter paper and kept aside unperturbed in a dust free room for the growth of single crystal. A good transparent needle shaped crystals was harvested in a growth period of 25-30 days. The purity of the synthesized crystal was further improved by repeated recrystallization process using methanol as solvent. (Scheme 1)

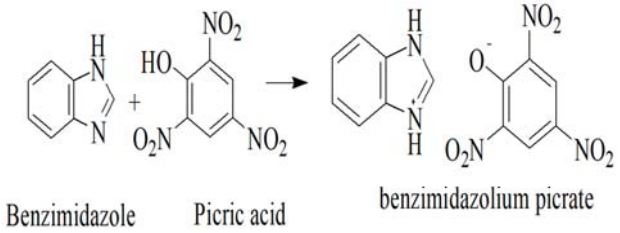

Synthesis of Benzimidazolium Picrate complex

Scheme 1

Antioxidant behaviour

The 2,2-diphenyl-2-picryl-hydrazyl radical scavenging activity of the compound was measured according to the method of Elizabeth & Rao[42]. The DPPH is a free radical having a stable λ_{max} at 517 nm. A fixed concentration of the experimental compound (100 µL) was added to a solution of DPPH in methanol (0.3 mM, 1 mL) and the final volume were made up to 4 mL with double distilled water. DPPH solution with methanol was used as a positive control and methanol alone acts as blank. The solution was incubated at 37°C for 30 min in darkness. The decrease in absorbance of DPPH was measured at 517 nm. The tests were run in triplicate and various concentrations (20-100 µg/ mL) of the compounds were used to fix a concentration at which the compounds showed 50% activity. In addition, the percentage of activity was calculated using the formula, % of suppression ratio = $[(A_0 - A_c)/A_0]$ X 100. Where, A_0 and A_c are the absorbance in the absence and presence of the tested compounds, respectively. The 50% activity (IC_{50}) can be calculated using the percentage of activity.

DNA binding experiments

The binding affinity of the compound with CT-DNA was carried out in double distilled water with tris(hydroxymethyl)-aminomethane (Tris, 5 mM) and sodium chloride (50 mM). The pH was adjusted to 7.2 using hydrochloric acid. A result of CT-DNA in the buffer gave a ratio of UV absorbance with reference to 1.8-1.9 at 260 and 280 nm, indicating that the DNA was suitably free of protein. The DNA concentration per nucleotide was determined by absorption spectroscopy using the molar extinction coefficient

value of 6600 dm^3 mol^{-1} cm^{-1} at 260 nm. The compound was dissolved in a mixed solvent of 5% DMSO and 95 % tris HCl buffer for all the experiments. Stock solutions were stored at 4°C and used within 4 days. Absorption titration experiments were performed with a fixed concentration of the compound (25 μM) with varying concentration of DNA (0-50 μM). While measuring the absorption spectra, an equal amount of DNA was added to all the test solutions and reference solution to eliminate the absorbance of DNA itself.

Results and Discussion

Elemental analysis

The transparency and constituents of elements (CHN) of the synthesized complex were verified by the elemental analysis. The results shows that the compound BP contains C: 43.20 (44.97%), H: 2.12 (2.61%), N: 19.91 (20.17%), O 31.25 (32.25%).The data analysed show that the experimentally obtained values are in good agreement with theoretical values (within the bracket). The result confirms the formation of the compound in stoichiometric proportion and the compound is free of impurities.

IR spectra

The characteristic vibrational frequencies of the functional group in the crystal lattice of BP are known through IR spectrum as shown in (Fig. 1) The formation of the charge transfer complex is strongly evidenced by the donor (picric acid) and acceptor (benzimidazole) molecules in the spectrum[43,44]. It is generally expected in acid – base interaction that there is a transfer of proton from the donor (acid) to acceptor (base). From the spectrum it is observed that the bands of the donor are slightly shifted to lower frequency and that of the acceptor are slightly shifted to higher frequency. This shift has been attributed to the charge transfer from the donor to acceptor upon the complexation. The band observed at 3155 cm^{-1} is due to the N^+-H stretching vibration.

The absorption peak at 3663 cm^{-1} is due to the N-H asymmetric stretching vibration and corresponding symmetric stretching vibration is observed at 3093 cm^{-1}. The aromatic C-H stretching vibration appears at 3055 cm^{-1}. The peak at 933 cm^{-1} is assigned to C-NO_2 stretching vibration. The frequencies at 1080 cm^{-1} is owed to C-H in plane bending vibration. The aromatic C=C stretching vibration is exhibited at 1604 cm^{-1}. The peak at 1527 cm^{-1} is due to NO_2 asymmetric stretching vibration and the corresponding symmetric stretching vibration band is observed at 1327 cm^{-1}. The band is at 709 cm^{-1} owes to the aromatic C-H out of plane bending vibration. The C-O stretching vibration appears at 1256 cm^{-1}. The NO_2 scissoring and wagging vibrations are observed at 840 and 748 cm^{-1}.

UV-visible absorption spectra

The optical absorption band is the most important parameter of the synthesised material for the implementation of various optical and biological applications. UV absorption spectra arise from the transition of electrons within a molecule from a lower electronic energy (LUMO) state to higher energy state (HOMO). When an atom or molecule absorbs the energy, electrons are promoted from their ground state to an excited state. The UV-visible absorption spectrum of the complex is shown in Fig. 2. The π-π∗ and n-π∗ transitions of BP appears 225 nm and 268 nm, respectively .The change in the band is due to the transfer of an electron from donor

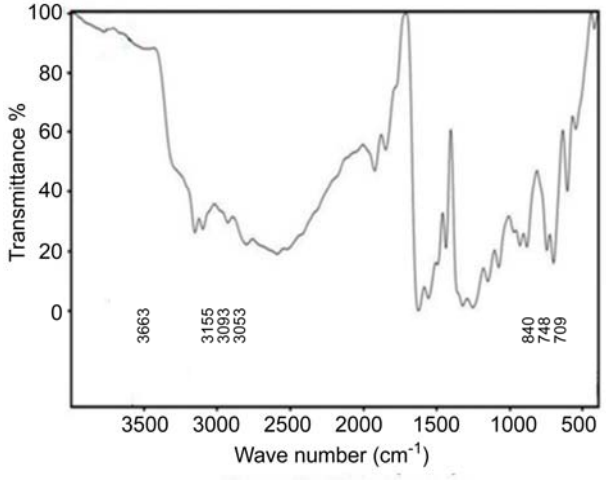

Fig. 1 — IR Spectrum of Benzimidazolium

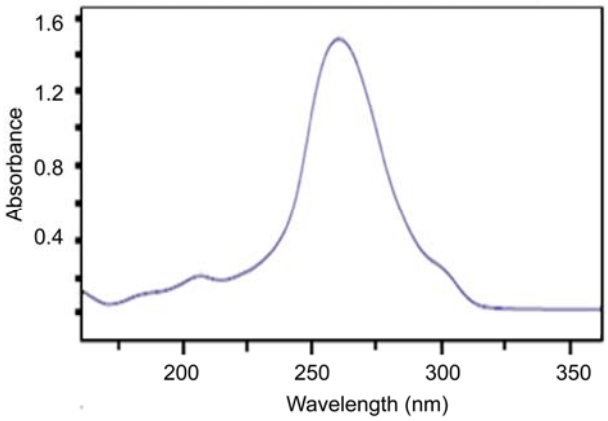

Fig. 2 — Electronic absorption spectrum of Benzimidazolium picrate

benzimidazole molecule to the acceptor picric acid molecule and appears on the longer wave length region. The charge transfer transition expected to occur in the longwave length region is gets submerged under the more intense n-π* band.

NMR spectra

Molecular structure and carbon skeleton of BP crystals were confirmed by ^{1}H and ^{13}C NMR studies resulting from dissolution of crystalline BP in deuterated methanol are shown in Fig. 3 A and B, respectively. Six dissimilar proton signals appeared in the spectrum, confirming the presence of six different proton environments in the BP system. The downfield signal at 9.5 ppm corresponds to protons (H6 and H5A) of the picrate anion. The most intense singlet peak at δ 8.9 ppm is assigned to the ring proton (H11) of the benzimidazolium moiety. The absence of any signal above δ 11 ppm impute to the phenolic proton confirming the existence of the picrate anion in solution through proton transfer mechanism. In the spectrum, the signals at δ 8.1 and (two H atoms attached to C_{13} and C_8) and δ 7.9 ppm (two H atoms attached to C_{12} and C_7) authenticate the presence of two sets of chemically equivalent protons in the aromatic ring of benzimidazolium moiety.

A singlet signal at δ 5 ppm is attributed to the -NH protons of benzimidazolium moiety in the BP complex. The carbon signal appeared in the upfield at δ 139.5 is attributed to the C_2 and C_{11} carbon atoms of BP. The weak carbon signal at δ 130 owes to the C_1, C_3 and C_4 carbon atoms in which nitro group is present in the picrate moiety. The C_5 and C_6 carbon atoms of the same kind bring forth a signal at δ 126.4. The highly intense peak at δ 125.1 is due to C_7, C_{12}/C_8, C_{13} carbon atoms of the same environment in benzimidazolium moiety and the signal at δ 45 is assigned to solvent carbon atom of the compound.

Thermal analysis

The thermal stability and its decomposition pattern of BP has been established by consecutively employing TG/DTA analysis and the thermogram is shown in Fig. 4. From TG curve, it is contained that the title complex is stable up to 146°C and it decompose immediately after melting which is inferred that there is no inclusion of environmental moisture during crystallization. The decomposition occurs in a single stage. From the DTA curves, the sharp endothermic peak appearing at 146°C

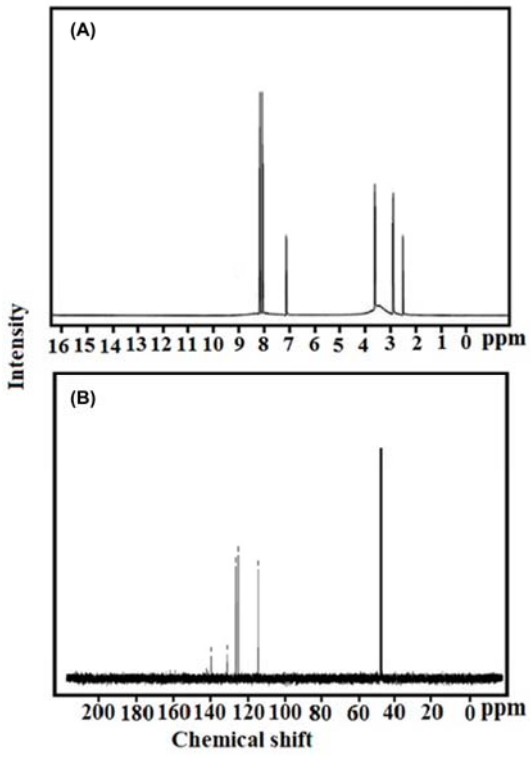

Fig. 3 — (A) ^{1}H NMR spectrum and (B) ^{13}C NMR of BP

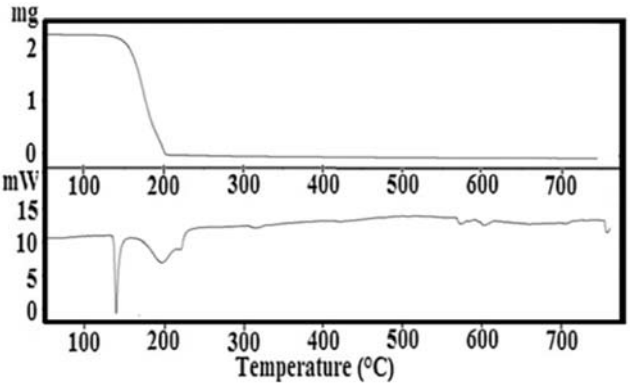

Fig. 4 — Thermal analysis graphs of BP

corresponds to the melting point of the material. This is followed by endothermic may be possible due to complex formation. No thermal anomaly was observed before the 146°C, this suggests that the BP was stable up to 146°C.

DNA binding studies

Electronic absorption spectroscopy is one of the most common and effective technique for investigation of the binding modes of organic compounds with CT-DNA. Compound binding through intercalation usually results in hypochromism with or without small red or blue shift, since the

intercalative mode involves a strong interaction between the aromatic chromophore and the base pairs of DNA[45]. Absorption spectra of the BP in the absence and presence of CT-DNA is given in (Fig. 5).

The binding mode of BP has been characterized through absorbance and shifts in the wavelength as a function of added concentration of DNA. Upon addition of increasing amounts of CT-DNA, a significant hypochromism is observed. This can be attributed to a strong interaction between DNA and compound and it is also likely that this compound binds to the DNA helix *via* intercalation. In order to illustrate quantitatively the consequence, the absorption data were analyzed to evaluate the intrinsic binding constant (K_b), which can be determined from the following equation [46-48],

$$DNA/ (\varepsilon_a - \varepsilon_f) = [DNA]/ (\varepsilon_b - \varepsilon_f) + 1/K_b (\varepsilon_b - \varepsilon_f)$$

where [DNA] is the concentration of DNA in base pairs, the apparent absorption coefficient ε_a, ε_f and ε_b corresponds to A_{obs}/[compound], the extinction coefficient of the free compound and the extinction coefficient of the compound when fully bound to DNA, respectively. From the plot of DNA/(ε_a- ε_f) versus [DNA], K_b is calculated by the ratio of slope to the intercept. The magnitude of intrinsic binding constant (K_b) value for BP is 4.9 X 10^4 M^{-1}. From the above DNA binding results, it is obvious that the title compound has planarity and extended π system which lead to the possibility of DNA intercalation.

Antioxidant activity

The DPPH radical has been used to test the ability of compound as free radical scavenger or hydrogen donor to evaluate the antioxidant activity. Hence experiments were carried out to explore the free radical scavenging ability of benzimidazolium picrate with DPPH radical[49,50] and compared with those of the positive control, ascorbic acid (Aca). The compound shows significant capacity for scavenging DPPH and the IC_{50} value (Fig. 6) indicated that it shows potent antioxidant activity. It also shows scavenging capacity beyond 83 μm/mL. The activity of BP is also found to be good. **(**Table 1**)**

Single crystal X-ray diffraction method

A single crystal X-ray analysis is made at 296 K using suitable crystals for data collection. Accurate lattice parameters are resoluted from least squares refinement of well centered reflection in the range 2.58 θ U θ 28.30. The complex, BP belongs to the monoclinic system with space group $P2_1/c$. The lattice

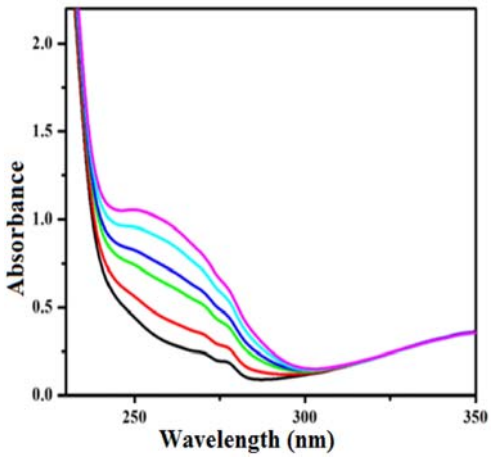

Fig. 5 — Electronic spectra of BP in Tris–HCl buffer upon addition of CT-DNA

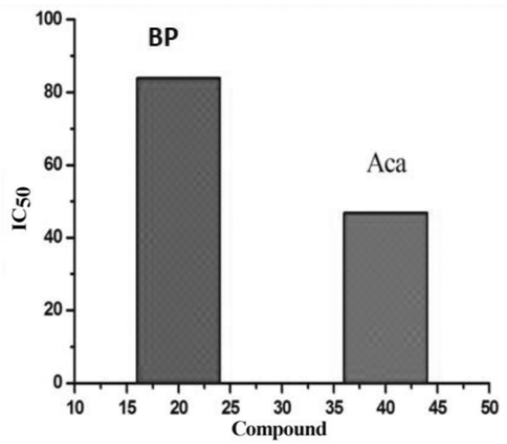

Fig. 6 — Antioxidant activity of BP

[Compound] = 25 μM, [DNA] = 0–50 μM DNA Solvent = (95% Water and 5%DMSO) (Inset: Plot between [DNA] and [DNA]/[ε_a–ε_f]X 10^{-8})

Table 1 — Comparison of antioxidant activity of Benzimidazolium picrate (BP) with other compounds

Compound	DPPH activity IC_{50}%
2-Amino-4-methoxy-6-methylpyrimidine[49]	55
2,3-dimethylquinoxalinium-p-toluenesulfonate[50]	110
3-aminopyridium- p-toluenesulfonate[51]	125
Benzimidazolium picrate	83
Ascorbic acid	66.26

parameter obtained are a=9.2376(7) Å, b=11.9355(7) Å, c= 12.8931(7) Å, α =90.00°, β=97.811(2)°, γ=90.00° and the unit volume is 1408.34(16) $Å^3$. The crystallographic data and structure refinements of BP complex are given in Table 2.

The benzimidazolium ion appears in crystalline lattice as single protonated cation and the picrate ion

Table 2 — Crystallographic data and structure refinement parameters of Benzimidazolium picrate (BP) complex

Empirical formula	C_{13} H_9 N_5 O_7
Formula weight	347.25
Temperature	296 (2) K
Wavelength	0.71073 Å
Crystal system	Monoclinic
Space group	$P2_1/c$
Cell dimensions	a = 9.2376(7)Å, α =90.00° b = 11.9355(7) Å, β = 97.811(2)° c = 12.8931(7) Åγ = 90.00°
Volume	1408.34(16) $Å^3$
Z	4
Density (calculated)	1.638 mg/m^{-3}
Absorption coefficient	0.137 mm^{-1}
$F_{(000)}$	712
Crystal size	0.40 × 0.35 × 0.30 mm^{-1}
Reflections collected	11222
Range for data collection (deg)	2.58-28.30 °
Number parameters	227
Absorption correction	Semi-empirical from equivalents
Max and min. transmission	0.9602 and 0.9474
Limiting indices h, k, l	-12/8, -15/15, -17/15
Refinement method	Full-matrix least squares on F^2
Goodness of F^2	1.017

is present as deprotonated anion. X-ray single crystal structure of the charge-transfer complex of benzimidazole with picric acid shows the presence of mono protonated benzimidazolium cation and gives the intermolecular hydrogen bonding association. The ORTEP diagram of BP is depicted the Fig. 7.

The selected bond lengths and bond angle is given in Table 3, respectively. In the picrate anion, C-O bond distance of anion is evident for characteristic values with C2–O6 [1.2413(18) Å] which is intermediate between single and double bond characters. The loss of a proton from picric acid is confirmed by the lengthening of the C-C bonds. The C1-C2 and C1-C3 bond lengths are (1.447(2) Å) and (1.450(2) Å), respectively which deviate from the standard aromatic C-C bond length (1.40 Å). These differences are attributed to the loss of a hydroxyl proton at O6, leading to conversion from neutral to the anionic state where the negative charge is constrained to lie in the ring. The crystal packing diagram of BP is shown in Fig. 8.

The picrate anion plays a vital role in forming hydrogen bonds with cation and stabilizing the structure. The degree of twisting of the nitro group from the benzene plane does not depend upon the C-N bond distance. The C-O bond length of the phenolate [1.248(2)°] corresponds to a partial double bond

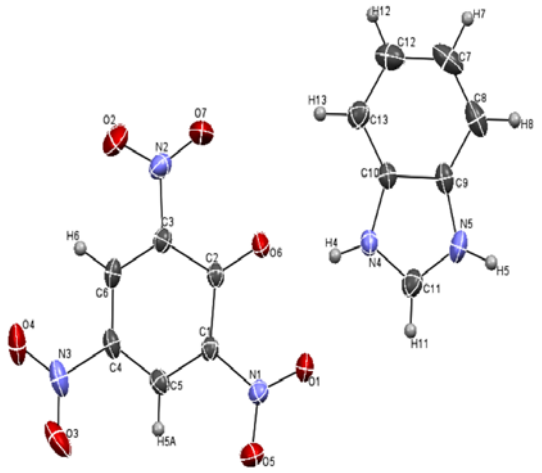

Fig. 7 — ORTEP diagram of BP

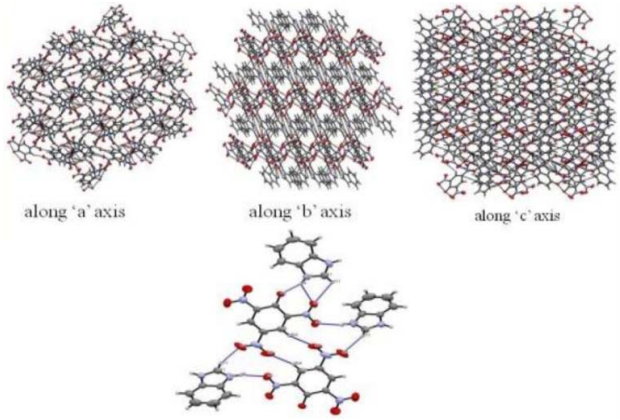

Fig. 8 — Crystal packing diagram of BP

character implying that the negative charge located on the phenolate oxygen atom is delocalized. The N-O bond distance of the nitro groups of the trinitro-phenolate anion are typical double bonds.

The twist angles of the three nitro group from the benzene plane of the picrate ion are (O1-N1-O5, 121.10(14) Å), (O7-N2-O2, 121.68(17) Å) and (O3-N3-O4, 123.24(17) Å). Analysis of the picrate ion show that the ortho nitro groups in general, deviate away from the benzene plane due to steric interactions with the phenol group at C5 but para nitro group lies in the benzene plane. Deviation from the normal behaviour arises in many structures as a result of crystal packing criteria which involve N-H...O and C-H....O hydrogen bonds with the nitro group O atoms.

The formation of intermolecular hydrogen bond N-H....O and C-H....O in crystal structure lead to supramolecular networking. The hydrogen bonded networks of the BP indicates that the cation part

Table 3 — Selected bond length (Å) and bond angle (°) of BP complex

Atom	observed	Atom	Observed	Atom	observed
O(1)-N(1)	1.2188(18)	C(10)-C(13)	1.381(2)	C(5)-C(4)-N(3)	119.36(16)
O(2)-N(2)	1.214(2)	C(11)-H(11)	0.93	C(6)-C(4)-N(3)	119.01(16)
O(3)-N(3)	1.217(2)	C(12)-C(13)	1.363(3)	C(4)-C(5)-C(1)	118.94(15)
O(4)-N(3)	1.229(2)	C(12)-H(12)	0.93	C(4)-C(5)-H(5A)	120.5
O(5)-N(1)	1.2345(18)	C(13)-H(13)	0.93	C(1)-C(5)-H(5A)	120.5
O(6)-C(2)	1.2413(18)	O(1)-N(1)-O(5)	121.10(14)	C(3)-C(6)-C(4)	119.52(15)
O(7)-N(2)	1.187(2)	O(1)-N(1)-C(1)	120.80(14)	C(3)-C(6)-H(6)	120.2
N(1)-C(1)	1.444(2)	O(5)-N(1)-C(1)	118.09(14)	C(4)-C(6)-H(6)	120.2
N(2)-C(3)	1.456(2)	O(7)-N(2)-O(2)	121.68(17)	C(8)-C(7)-C(12)	122.5(2)
N(3)-C(4)	1.441(2)	O(7)-N(2)-C(3)	120.28(16)	C(8)-C(7)-H(7)	118.7
N(4)-C(11)	1.312(2)	O(2)-N(2)-C(3)	118.03(16)	C(12)-C(7)-H(7)	118.7
N(4)-C(10)	1.381(2)	O(3)-N(3)-O(4)	123.24(17)	C(7)-C(8)-C(9)	116.29(19)
N(4)-H(4)	0.86	O(3)-N(3)-C(4)	118.99(18)	C(7)-C(8)-H(8)	121.9
N(5)-C(11)	1.320(2)	O(4)-N(3)-C(4)	117.76(19)	C(9)-C(8)-H(8)	121.9
N(5)-C(9)	1.381(2)	C(11)-N(4)-C(10)	108.82(14)	N(5)-C(9)-C(8)	132.91(17)
N(5)-H(5)	0.86	C(11)-N(4)-H(4)	125.6	N(5)-C(9)-C(10)	105.98(15)
C(1)-C(5)	1.373(2)	C(10)-N(4)-H(4)	125.6	C(8)-C(9)-C(10)	121.11(19)
C(1)-C(2)	1.447(2)	C(11)-N(5)-C(9)	108.82(14)	N(4)-C(10)-C(13)	131.23(15)
C(2)-C(3)	1.450(2)	C(11)-N(5)-H(5)	125.6	N(4)-C(10)-C(9)	106.38(15)
C(3)-C(6)	1.356(2)	C(9)-N(5)-H(5)	125.6	C(13)-C(10)-C(9)	122.39(17)
C(4)-C(5)	1.369(2)	C(5)-C(1)-N(1)	115.95(14)	N(4)-C(11)-N(5)	110.01(16)
C(4)-C(6)	1.381(2)	C(5)-C(1)-C(2)	124.01(14)	N(4)-C(11)-H(11)	125
C(5)-H(5A)	0.93	N(1)-C(1)-C(2)	120.04(13)	N(5)-C(11)-H(11)	125
C(6)-H(6)	0.93	O(6)-C(2)-C(1)	124.88(14)	C(13)-C(12)-C(7)	121.7(2)
C(7)-C(8)	1.358(3)	O(6)-C(2)-C(3)	123.06(14)	C(13)-C(12)-H(12)	119.1
C(7)-C(12)	1.393(4)	C(1)-C(2)-C(3)	112.02(13)	C(7)-C(12)-H(12)	119.1
C(7)-H(7)	0.93	C(6)-C(3)-C(2)	123.90(15)	C(12)-C(13)-C(10)	115.93(18)
C(8)-C(9)	1.383(3)	C(6)-C(3)-N(2)	116.19(14)	C(12)-C(13)-H(13)	122
C(8)-H(8)	0.93	C(2)-C(3)-N(2)	119.89(14)	C(10)-C(13)-H(13)	122
C(9)-C(10)	1.386(2)	C(5)-C(4)-C(6)	121.60(14)		

joined to the anion part via extended hydrogen bonding. In crystal structure the cation and anion linking by strong N-H...O and C-H....O hydrogen bonding. The combination of all type of inter-molecular hydrogen forms three dimensional networks. This hydrogen bonding link layer of cation with the layer anion form straight chain along in the b axis.

Conclusions

A novel organic charge transfer crystal of Benzimidazolium picrate was synthesized and successfully grown by the slow evaporation solution growth technique at ambient temperature. The single crystal analysis indicated that the crystal belongs to monoclinic with P21/c space group. The CT complex is found to be biologically significant with regards to its DNA binding. The radical scavenging activity showed that the CT complex possesses the greater activity against DPPH radical. FTIR was substantial the presence of functional group, especially $^{+}$NH stretching vibration at 3155 cm^{-1}. The UV spectrum confirmed the formation of CT complex. TG and DTA analysis inferred the thermal stability of the synthesized complex. The proton and carbon positions were analyzed by NMR spectra which establish molecular structure of the crystal.

Acknowledgement

The authors acknowledge STIC Cochin for single crystal XRD and Kovai Medical Centre and Hospital Coimbatore for assistance in carrying out the antioxidant activity.

Conflict of interest

The authors declare no conflict of interests in this study.

References

1 Cassemiro BG, SantosWillian JS, Oliveira XC, Pereira-Maia EC, Galvao BRL, do Pim WD & Silva-Caldeira PP, *Appl Organomet Chem* 34 (2020) 5425.

2 Santosh PC, Pandeya SN & Pathak AK, *Int J Res Ayurveda Pharm*, 2 (2011) 1726.

3 Nannapaneni DT, Gupta A, Reddy MI & ChSarva R, *J Young Pharm*, 2 (2010) 273.

4 Nakano H, Inoue T, Kawasaki N, Miyataka H, Matsumoto H, Taguchi T, Inagaki N, Nagai H & Satoh T, *Bioorg Med Chem*, 8 (2000) 373.
5 Zhao ZS, Arnaiz DO, Griedel B, Sakata S, Dallas JL, Whitlow M, Trinh L, Post J, Liang A, Morrissey MM & Shaw KJ, *Bioorg Med Chem Lett*, 10 (2000) 963.
6 White AW, Almassy R, Calvert AH, Curtin NJ, Griffin RJ, Hostomsky Z, Maegley K, Newell DR, Srinivasan S & Golding BT, *J Med Chem*, 43 (2000) 4084.
7 Zhu Z, Lippa B, Drach JC & Townsend LB, *J Med Chem*, 43 (2000) 2430.
8 Kalarani R, Sankarganesh M, Vinoth Kumar GG & Kalanithi M, *J Mol Struct*, 1206 (2020) 127725.
9 Chinnaraj A, Murugesan S, Jeyaraj DR & Manivannan K, *J Serb Chem Soc*, 84 (2019) 267
10 Khargonekar P, Sinskey A, Miller C & Ranganathan B, *Cancer Sci Res*, 4 (2017) 1.
11 Shanmugavel M, Vasantharaj S, Yazhmozhi A, Bhavsar P, Aswin P, Felshia C, Mani U, Ranganathan B & Gnanamani A, *Biocatal Agric Biotechnol*, 15 (2018) 295
12 Ranganathan B, *Res Ind*, 40 (1995) 342
13 Greenhill JV & Lue L, *Prog Med Chem*, vol. 30, (Eds. GP Ellis & DK Luscombe, Elsevier, New York), 1993, pp 170.
14 Preston PN, *Chem Rev*, 74 (1974) 179.
15 Touzeau F, Arrault A, Guillaumet G, Scalbert E, Pfeiffer B, Rettori MC, Renard P & Merour JY, *J Med Chem*, 46 (2003) 1962.
16 Roundu F, Bihan GL, Wang X, Lamouri A, Touboul E, Dive G, Bellahsene T, Pfeiffer B, Renard, P, Guardiola-Lemaitre B, Maneche D, Penicaud L, Ktorza A & Godfroid, JJ, *J Med Chem*, 40 (1997) 3793.
17 Vadivelan G, Saravanabhavan M, Murugesan V, Gohulvani G, Sekar M & Babu B, *Mol Cryst Liq Cryst*, 652 (2017) 242.
18 Weller A & Zachariasse K, Chemiluminescence from Radical Ion Recombination VI. Reactions, Yields, and Energies. In: *Chemiluminescence and Bioluminescence*, (Ed. Cormier M; Springer, NY, USA), 1973, pp 181.
19 Gupta RK & Singh RA, *J Appl Sci*, 5 (2005) 28.
20 Hashem HA & Refat MS, *Surf Rev Lett*, 13 (2006).
21 Tracz, *Polym J Chem*, 76 (2002), 457.
22 Ishaat IM & Ahmed A, *Spectrochim Acta A*, 77 (2010) 437.
23 Yasutake M, Araki K, Zhou M, Nogita R & Shinmyozu T, *Eur J Org Chem*, 7 (2003) 1343.
24 Gutmann F, Johnson C, Keyzer H & Molnar J, *Charge Transfer Complexes in Biochemistry System*, 1st Edn., (CRC Press, FL, USA), 1997.
25 Palacios RE, Kodis G, Gould SL, Garza de la L, Brune A, Gust D, Moore TA, *Chem Phys Chem*, 6 (2005) 2359.
26 Chemla DS & Zyss J, *Nonlinear optical properties of organic molecules and crystals*, *vols. 1 and 2*, (Academic Press, New York, USA), 1987.
27 Marcy HO, Rosker M J, Warren LF, Cunningham PH, Thomas CA, Deloacn LA, Velsko SP, Ebbers CA, Liao JH & Kantzidis MG, *Opt Lett*, 20 (1995) 252.
28 Wang XQ, Xu D, Yuan DR, Yu WT, Sun SY, Yang ZH, Fag Q, Lu K, Yan YX, Meng FQ, Guo SY, Zhang GH & Jiany MH, *Mater Res Bull*, 34 (1999) 2003.
29 Duan XL, Yuan DR, Wang XQ, Cheng XF, Yang ZH, Guo SY, Sun HQ & Klu XM, *Cryst Res Technol*, 37 (2002) 446.
30 Bock H, Nagel N & Seibel A, *Euro J Org Chem*, 1997 (2006) 2151.
31 Murugan E, Geetha Rani DP, Srinivasan K & Muthumary J, *Expert Opin Drug Deliv*, 10 (2013) 1319.
32 Murugan E, Arumugam S & Panneerselvam P, *Int J Polym Mater*, 65 (2016) 111
33 Murugan E, Gopinath P, Shanmugayya V & Mathivanan N, *J Appl Poly Sci*, 117 (2010) 3673.
34 Imai Y, Kamon K, Kinuta T, Sato T, Tajima N, Kuroda R & Matsubara Y, *Eur J Org Chem*, 2009 (2009) 2519.
35 Imai Y, Kamon K, Kido S, Sato T, Tajima N, Kuroda R & Matsubara Y, *Eur J Org Chem*, 2008 (2008) 4784.
36 Kusama H, Sugihara H, *J Photochem Photobiol A*, 181 (2006) 268.
37 In Y, Nagata H, Doi M, Ishida T & Wakahara A, *Acta Crystallogr C*, 53 (1997) 367.
38 Vogel AI, *Textbook of Practical Organic Chemistry*, 5th ed., (Longman, London), 1989.
39 Sheldrick GM, *Softerware for the CCD Detector System*, Bruker Analytical X-ray System Inc., Madison, WI, 1998.
40 Sheldrick GM, *SADABS*, A Program for Absorption Correction with the Siemens SMART Area Detector System, University of Gottingen, Germany, 1996.
41 Sheldrick GM, *SHELXS-97*, A Program for Solution of Crystal Structures, University of Gottingen, Germany, 1997.
42 Elizabeth K & Rao MNA, *Int J Pharmaceut*, 58 (1990) 237.
43 Elmosallamy MAF, *Anal Sci*, 20 (2004) 285.
44 Pashchevskaya NV, Nazarenko MA, Bolotin SN, Oflidi AI & M Panyushkin VT, *Russ J Inorg Chem*, 55 (2010) 1425.
45 Liu ZC, Wang BD, Li B, Wang Q, Yang ZY, Li TR & Li Y, *Eur J Med Chem*, 45 (2010) 5353.
46 Wolfe A, Shimer GH & Meehan T, *Biochemistry*, 26 (1986) 6392.
47 Sathiyaraj S, Sampath K, Butcher RJ, Jayabalakrishnan C, *Transition Met Chem*, 38 (2013) 291.
48 Sathiyaraj S, Sampath K, Butcher RJ, Pallepogu R, Jayabalakrishnan C, *Eur J Med Chem*, 64 (2013) 81.
49 Khamees HA, Yasser HE. Mohammed YHE, Swamynayaka A, Al-Ostoot FH, Sert Y, Alghamdi S, Khanum SA & Madegowda M, *Chem Select*, 4 (2019) 4544.
50 Parthasarathy K, Ponpandian T & Praveen C, *Chin J Catal*, 38 (2017) 775.